UCRL-84578
PREPRINT

SUPERNOVA MODELS AND LIGHT CURVES

Thomas A. Weaver
Lawrence Livermore Laboratory
Livermore, CA 94550

S. E. Woosley
University of California, Santa Cruz
Santa Cruz, CA 95064
and
Lawrence Livermore Laboratory
Livermore, CA 94550

This paper was prepared for submittal to
proceedings for the workshop on
Atomic Physics and Spectroscopy for Supernovae Spectra
La Jolla Institute
January 10-12, 1980

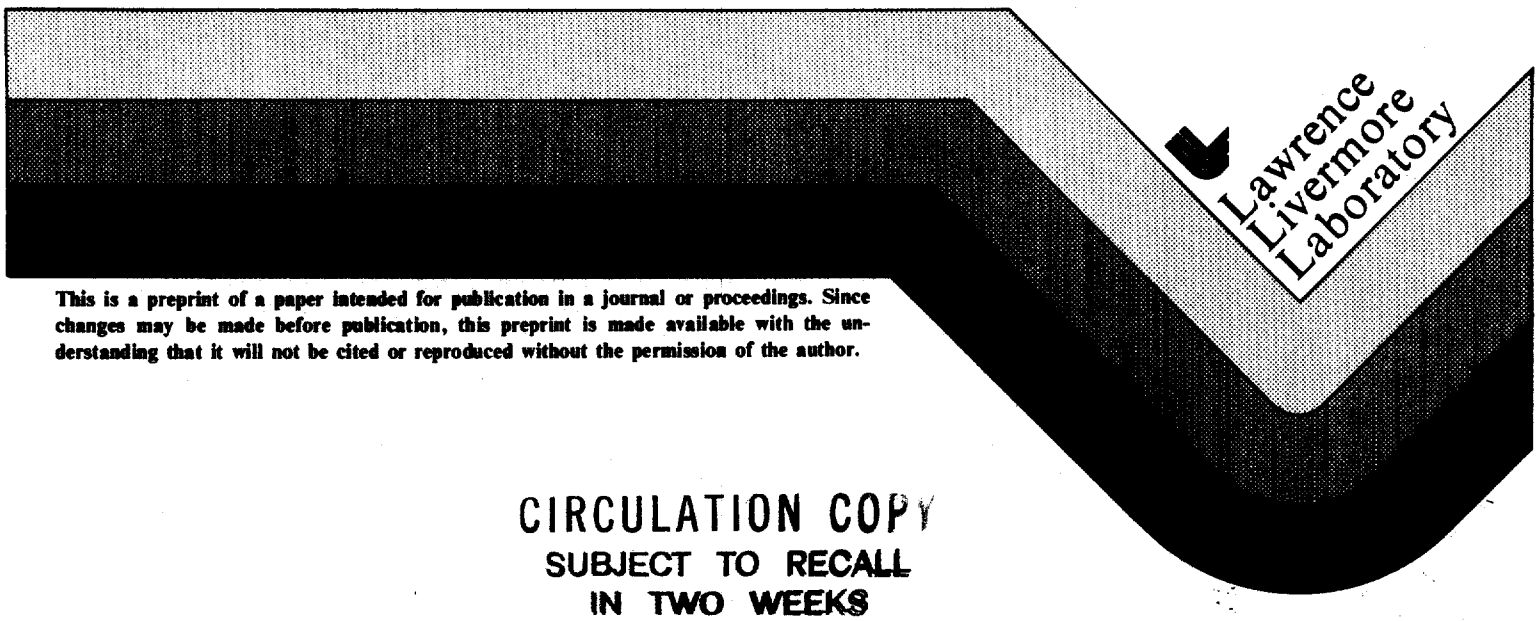

SUPERNOVA MODELS AND LIGHT CURVES*

Thomas A. Weaver
Lawrence Livermore Laboratory
Livermore, CA 94550

S. E. Woosley†
University of California, Santa Cruz
Santa Cruz, CA 95064
and
Lawrence Livermore Laboratory
Livermore, CA 94550

ABSTRACT

This talk briefly reviews the current status of our understanding of Type II supernovae with particular emphasis on the processes responsible for the emission of electromagnetic radiation. In addition, a relatively novel evolutionary scenario that appears to lead to a Type I supernova explosion is presented.

TYPE II SUPERNOVAE

Type II supernova have long been associated with massive stars with extended hydrogen envelopes. This association is due both to direct spectroscopic evidence[1,2,3] and to the quite distinct correlation of Type II supernovae with the spiral arms of galaxies[4], suggesting that their progenitors are bright, short-lived (<30 million years) O and/or B stars with mass $\geq 10\ M_{\odot}$.

We[5-8] have approached this issue from the theoretical viewpoint of evolving massive stars from the zero-age main sequence, through their various hydrostatic and explosive nuclear burning phases, and then comparing the characteristics of the supernova explosions that result to observations. Our numerical model[5] of these events incorporates implicit hydrodynamics with time-dependent convection and semiconvection, and a careful treatment of the complex nuclear processes that characterize the advanced nuclear burning stages. Spherical symmetry, and thus the absence of rotation and magnetic fields, is assumed, as is the unimportance of mass loss.

Complete evolutionary calculations have been performed for 15 and 25 $M_{\odot}$ Population I stars, and have been summarized by Weaver and Woosley[6]. (See Ref. 5, 6, and 7 for a discussion of the relation of these calculations to previous work.) We shall concentrate in this talk on the observable effects of the explosive death of these stars.

*Work performed under the auspices of the U.S. Department of Energy by LLNL under contract number W-7405-ENG-48.

†Work performed in part under NSF contract number AST-79-09102.

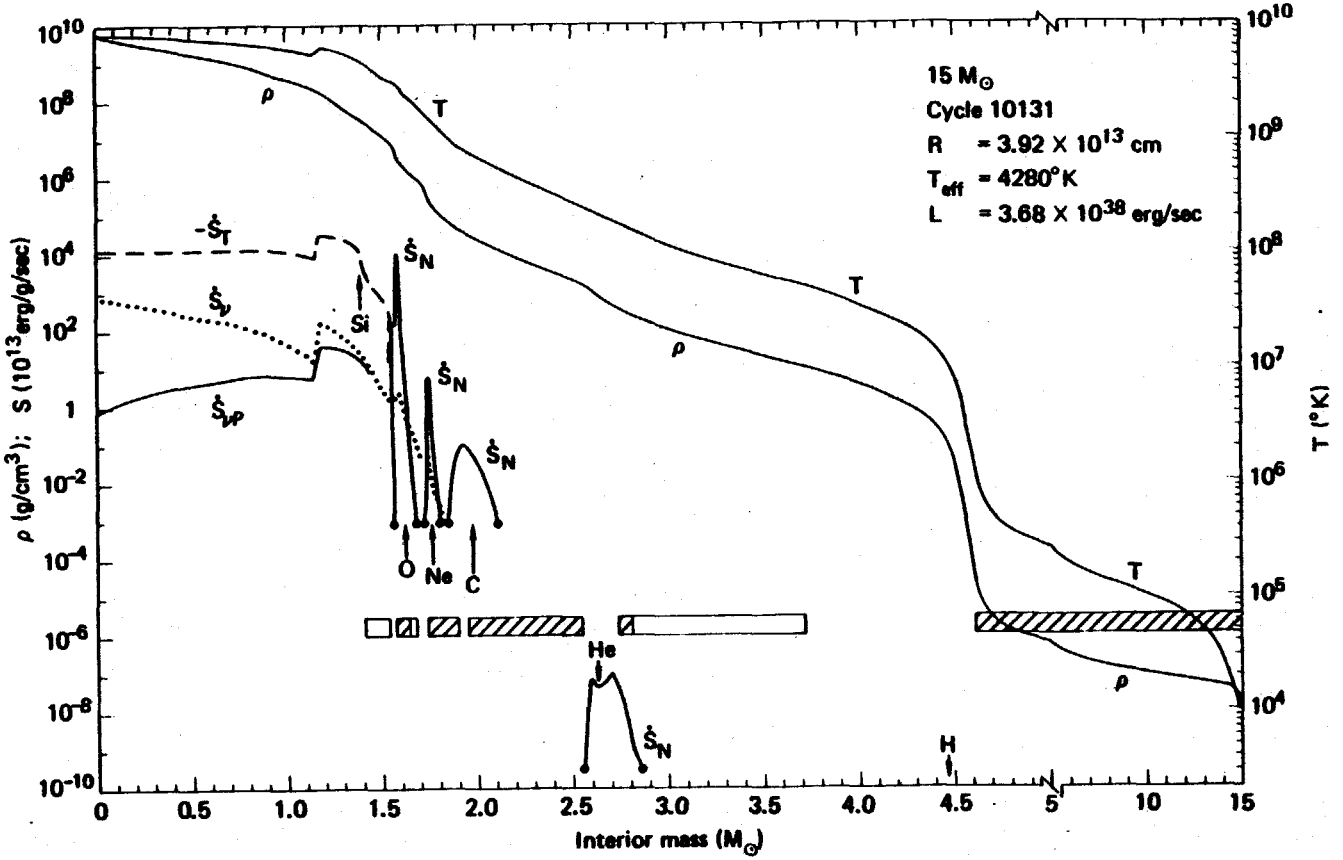

Fig. 1 The thermodynamic structure of the presupernova 15 $M_\odot$ model star is shown as a function of mass fraction.[5] Note that the density and temperature profiles are plotted such that the curves will maintain constant separation for the case $\rho \propto T^3$. Here $-\dot{S}_T$ is the total local energy loss rate due to both neutrino emission and nuclear photodisintegration, $\dot{S}_\nu$ is the total neutrino energy loss rate, and $\dot{S}_{\nu P}$ is the neutrino energy loss rate due to the thermal plasma processes. The nuclear energy generation rate profiles for the various nuclear burning shells are labelled $\dot{S}_N$, and the principal nuclear fuel is indicated. All energy generation and loss rates share the common scale denoted by "S". Active convective regions are indicated by striped bars, while semi-convective and convectively neutral regions are shown as outlined bars. In this figure, R, T_{eff}, and L denote the photospheric radius, effective temperature, and optical luminosity, respectively.

PRESUPERNOVA EVOLUTION

We find that the massive stars we have studied gradually deplete their store of nuclear fuel by burning their initially predominantly hydrogen composition successively into helium, carbon, neon, oxygen, silicon and finally iron. In general, each successive fuel is ignited in the star's core, while shells of the lighter elements remain in the region outside the core, usually separated by active nuclear burning shells. These burning shells are typically convective and are separated by sufficiently steep entropy gradients so that mixing between shells does not occur. The collapse of the core is triggered by the endothermic photodisintegration of iron[5] (c.f. Burbidge, Burbidge, Fowler, and Hoyle[9]). At this stage, about 2/3 of the star's mass resides in a tenuous red-supergiant envelope composed mostly of hydrogen (~60%) and helium (~40%), and having nearly constant 10^{-8}g cm^{-1} density and 10^5 K temperature (see Fig. 1 and Ref. 5). The radii of the 15 and 25 $M_\odot$ stars are respectively 4 and 7 x 10^{13} cm.

SHOCK WAVE PROPAGATION

The outgoing shock wave that is thought to result from the collapse and bounce of the core (c.f. Wilson[10]) can then (if sufficiently strong) eject the mantle and envelope of the star, while the core of the star recollapses to form a neutron star or black hole. This shock also induces explosive nuclear burning in the region just above the core, which though crucial to the synthesis of the elements in stars, adds only about 10 to 20% to the energy of the final supernova explosion. Much of the silicon layer directly over the iron core reaches temperatures above 4 billion degrees and is burned into 0.1 to 0.4 $M_\odot$ of radioactive ^{56}Ni (the most strongly bound nucleus that can be formed from the nearly equal numbers of neutrons and protons present in the initial fuel). ^{56}Ni, however, beta decays first to ^{56}Co and then to ^{56}Fe with a half-life of 6.1 and 78.5 days, respectively. The γ-rays and positrons that result from these decays represent an important late-time input to the thermal energy of the exploding star.

As the shock wave continues to propagate out through the mantle ($\rho \gtrsim 10$ g cm^{-1}) of the star, the energy needed to heat and accelerate each successive mass shell is smoothly derived from the subsonic deceleration and adiabatic decompression of the underlying material. Sensitivity tests[6] show that except in the immediate vicinity of the mass cut between the mantle and the collapsed core, only the observable final energy of the outward-going shock wave and not the details of its formation are important in determining postshock conditions for a given presupernova configuration. The entropy of the postshock material is roughly constant due to the approximate cancellation of the centrally depressed (by neutrino emission) presupernova entropy profile by the centrally peaked profile of entropy production by the shock (due to shock deceleration). Since sufficient

time is available for pressure balance to be established, this constant entropy profile results in nearly constant density and temperature profiles behind the shock front--in contrast to the thin, high density shells formed by a strong point explosion in an initially constant density medium.[11]

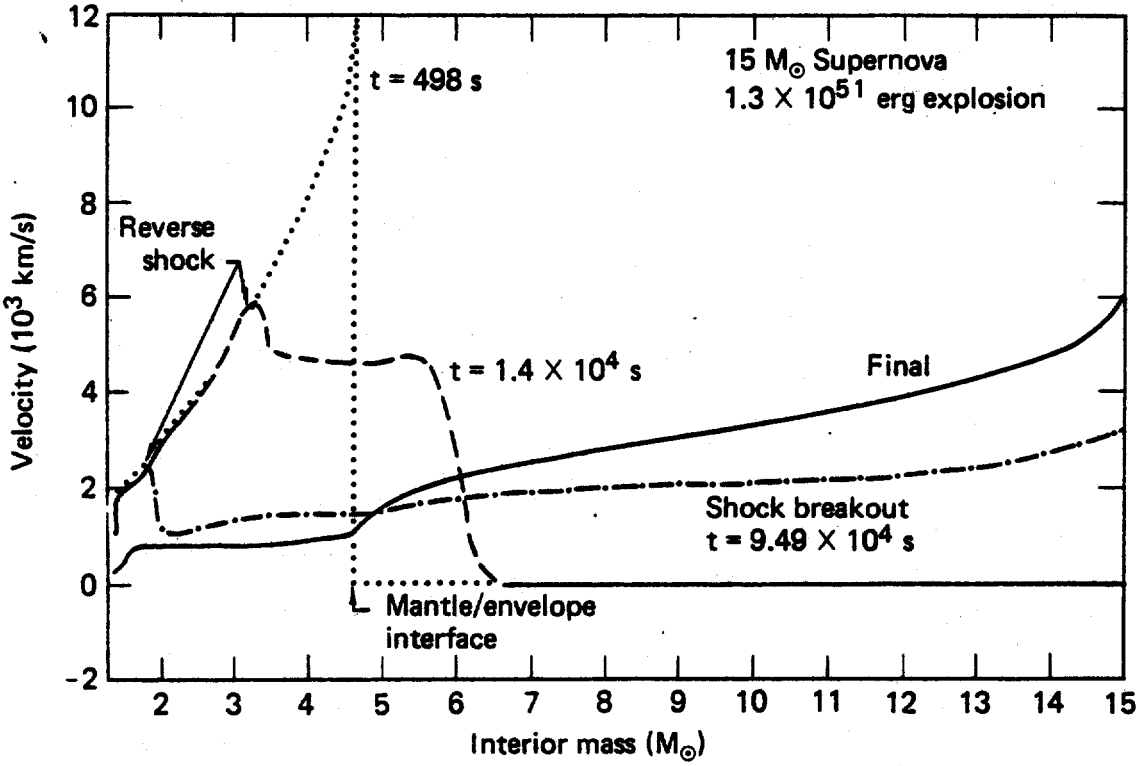

Fig. 2 Velocity as a function of interior mass coordinate in the 1.3 x 10^{51} erg, 15 $M_\odot$ supernova model at, and just after, the breakout of the shock wave from the surface. Each curve is labeled with the time in days since core collapse, and dotted line segments indicate regions with conditions allowing the growth of Rayleigh-Taylor instabilities.

Figure 2 details the hydrodynamical behavior of the mantle and envelope of our 15 $M_\odot$ model star undergoing a 1.3 x 10^{51} erg explosion (Model 15A, see Ref. 6). We shall discuss this case below as a typical Type II supernova because of its concordance with observation, and because 15 $M_\odot$ stars are observed to be more numerous than 25 $M_\odot$ stars[12], which we find to have generally similar behavior. During the time t=60-500 sec (measured from core collapse) the shock wave reaches and accelerates down the steep, 6-order-of-magnitude density gradient at the edge of the mantle, while the postshock material adiabatically expands and cools, initially unhindered by the surrounding low density envelope. By the time the exploding mantle has swept up sufficient envelope material to be significantly decelerated (t ~3,000 sec), its density has dropped to below 10^{-3} g cm^{-3} and its temperature below 2 x 10^6K. Under these conditions the expansion is hypersonic so that the deceleration of the mantle by the envelope is mediated by a reverse shock wave (see also Ref. 13).

This reverse shock has almost reached the center of the star when the principal shock wave reaches and accelerates down the final density gradient at the edge of the star at t=1.1 days. Subsequent adiabatic expansion over the next few days leads to the final velocity profile shown in Figure 2. Note that the velocity of the mantle has been reduced to below 1000 km/s both by the action of the reverse shock and the restraining pressure exerted by the decompressing envelope. The mantle, which contains virtually all the Z>2 elements synthesized by the star, including the ^{56}Ni, is thus left with only about 5% of total energy of the explosion.

Density and temperature profiles at, and just after, shock breakout are shown in Figures 3 and 4, and regions with conditions allowing the growth of Rayleigh-Taylor instabilities are indicated. In contrast to the more ad-hoc models studied by Chevalier and Klein[14], we find that most of the envelope is not subject to Rayleigh-Taylor instabilities during its acceleration. As pointed out by Lasher[15], however, the presence of such instabilities is likely to be a sensitive function of the density gradient in the convective red-giant envelope, and thus of our still incomplete understanding of superadiabatic convection.

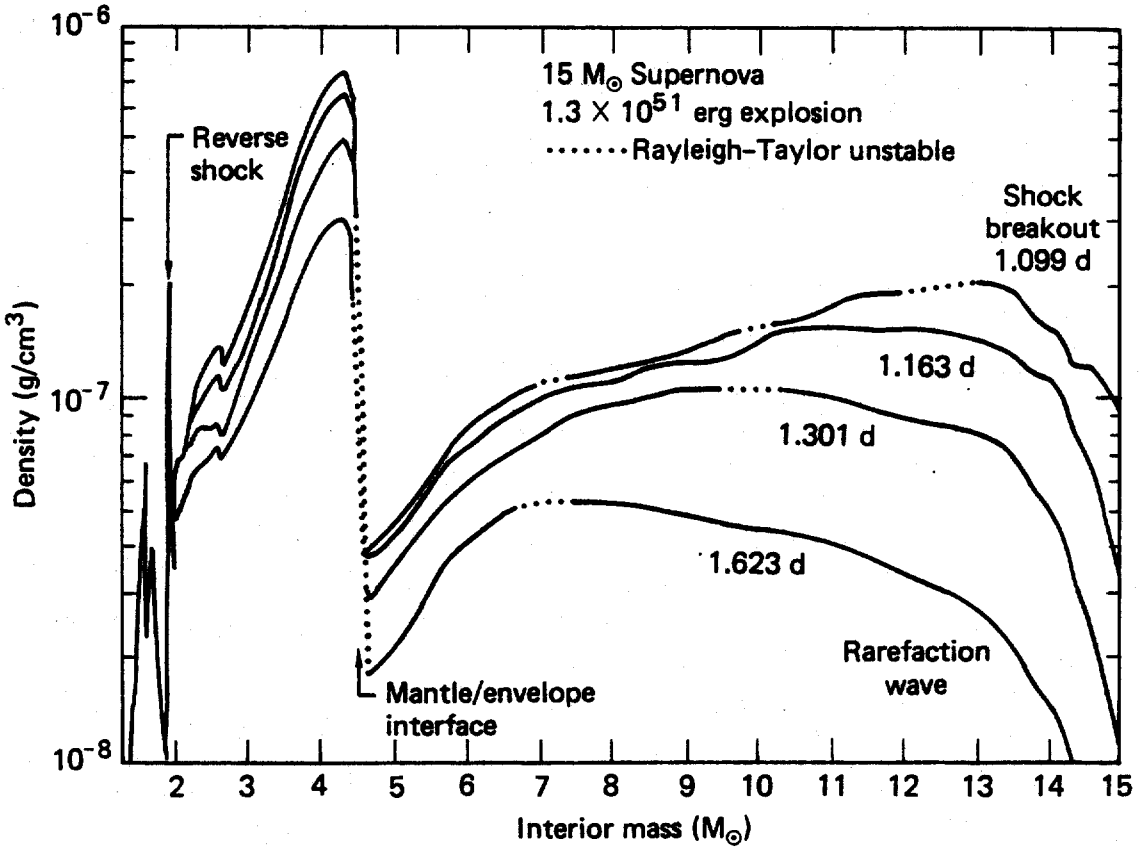

Fig. 3 Density as a function of interior mass coordinate in the 1.3 x 10^{51} erg, 15 $M_\odot$ supernova model at, and just after, the breakout of the shock wave from the surface. Each curve is labeled with the time in days since core collapse, and dotted line segments indicate regions with conditions allowing the growth of Rayleigh-Taylor instabilities.

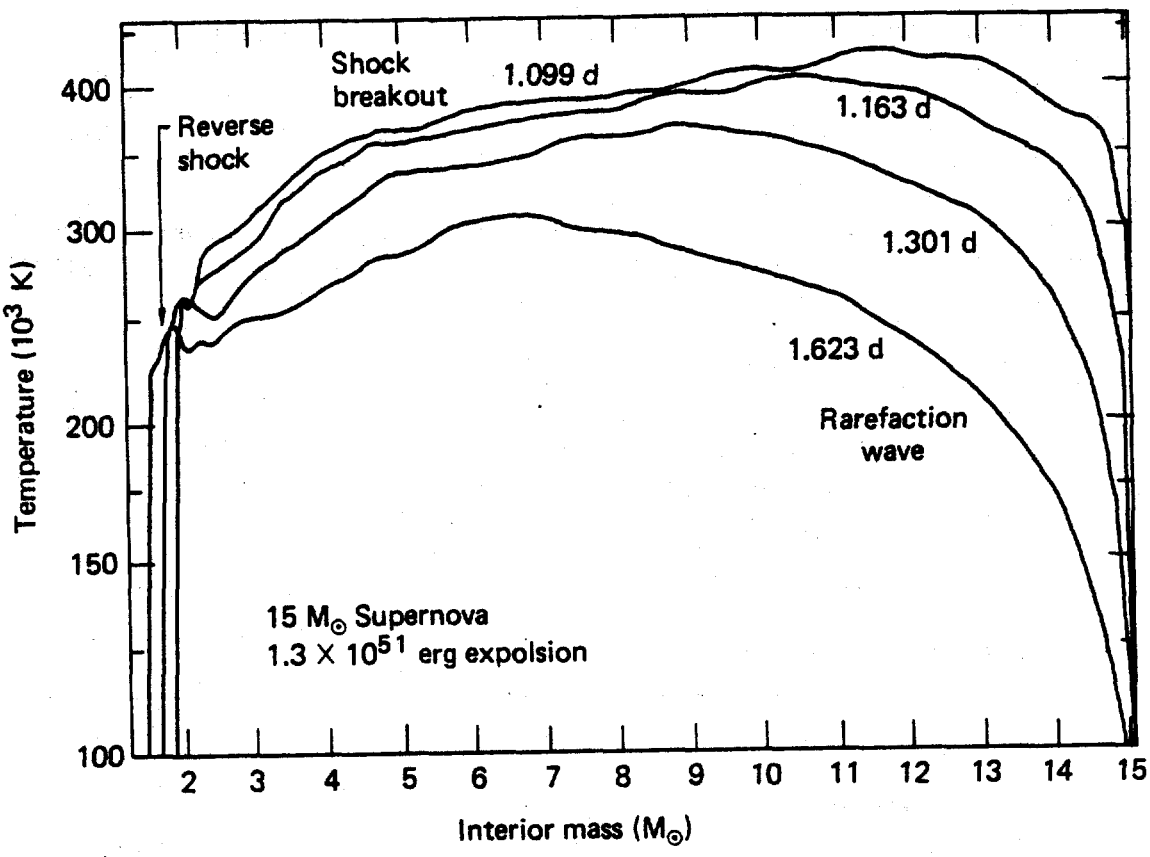

Fig. 4 Temperature profiles corresponding to the density profiles shown in Fig. 3.

TYPE II SUPERNOVA LIGHT CURVES

The light curves produced by two 15 $M_\odot$ supernova models (with differing explosion energies of 1.3 and 3.3 x 10^{51} ergs due to differing assumptions about detailed core physics) are shown in Figure 5, compared to photometric data for Supernova 1969ℓ in NGC 1058, perhaps the best observed Type II supernova.[2,16] SN 1969ℓ is characteristic of a common subclass of Type II supernovae which shows a 2-3 month initial plateau in its visual emission ($M_V \simeq -17$) followed by a rapid decline of about 2 stellar magnitudes and then a slower decline at a rate of ~3 magnitudes/year. (SN 1970g in NGC 5457=M101 is another recent example of this subclass).[17] It is apparent that the theoretical and observational results are in excellent agreement. As Figure 4 shows, an increase in the energy of the core explosion produces a roughly linear increase in the optical brightness together with a shorter "plateau". The results for our 25 $M_\odot$ models are generally quite similar. Note in particular that this agreement has not been achieved by normalizing the observational absolute magnitude so as to provide the best fit.

Figures 6 and 7 compare derived observational SN 1969ℓ results [2,16,18] for the temperature and radius of the supernova photosphere with the corresponding theoretical results. Figure 8 shows a comparison between observed absorption line velocities and photospheric

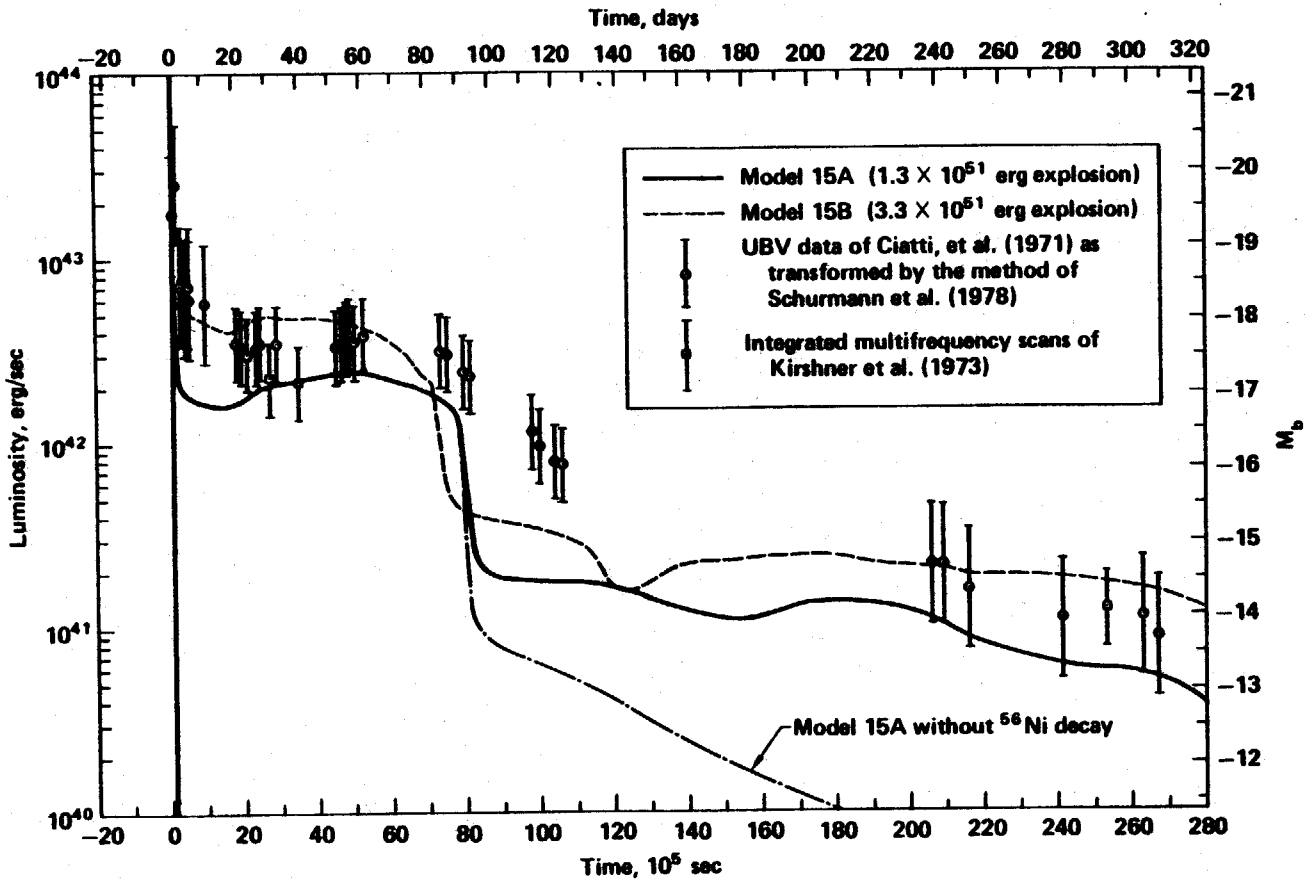

Fig. 5 Light curve of Type II supernova 1969ℓ compared to 15 $M_\odot$ theoretical models.[6] Here, M_b is the absolute bolometric magnitude of the supernova and time is measured with respect to core bounce for the theoretical models and Julian day 2,440,560 for the observations. The solid and dotted lines give the bolometric luminosity for the 15 $M_\odot$ models (15A and 15B), while the data points for 1969ℓ are either derived from the UBV data of Ciatti, et al.[16] as transformed by the method of Schurmann, et al.[21] (open circles) or obtained by integrating the multifrequency scans of Kirshner et al.[2] (open squares). The dot-dashed curve shows the result when ^{56}Ni decay is artificially suppressed in Model 15A.

velocities for the low energy 15 $M_\odot$ explosion. The agreement between theory and observation is uniformly within the observational errors, and allows a confident description of the general physical processes which are occurring (see also Ref. 13 and 19-22 for conclusions based on parameterized models).

The initial sharp spike in temperature and luminosity at small photospheric radius corresponds to the breakout of the supernova shock through the surface of the star's supergiant envelope. This is accompanied in theory[7,23-25] by a ~2000 second long, soft x-ray pulse with an equivalent black body temperature of ~1.5 x 10^5 K and a peak luminosity of ~10^{45} erg/second. The surface is then rapidly cooled by radiative emission and hydrodynamic expansion, balanced in part by radiative diffusion from below.

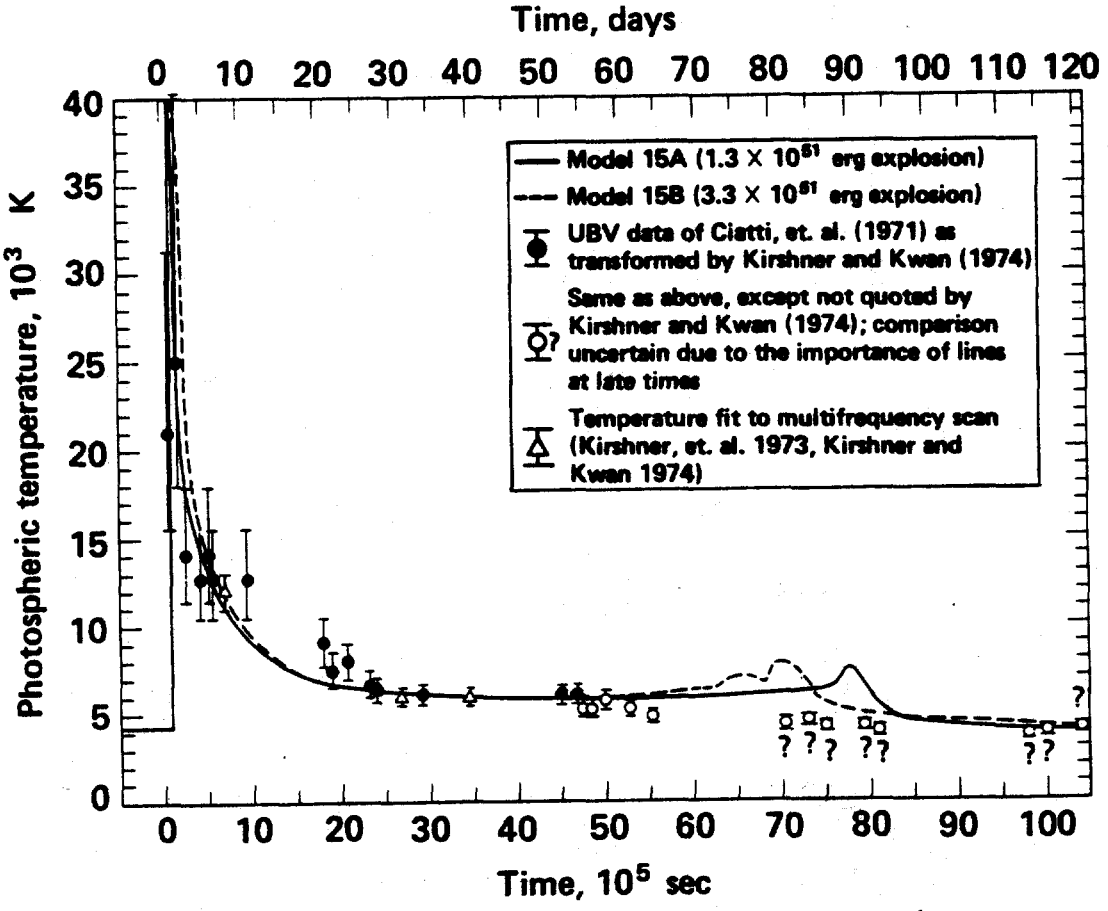

Fig. 6 Photospheric temperature of Type II supernova 1969ℓ compared with 15 $M_\odot$ theoretical models.[6] The solid and dotted lines give the results for the 15 $M_\odot$ models, while the solid circle data points represent the data of Ciatti, et al.[16] as transformed by Kirshner and Kwan.[18] The open circle data points are obtained by extrapolating the transformation methods of Kirshner and Kwan[18] to the late time data of Ciatti, et al.[16], and are associated with "?" marks where lines dominate the spectrum and such color/temperature transformations become dubious. The open triangle data points are derived from fits to multifrequency scans.[2]

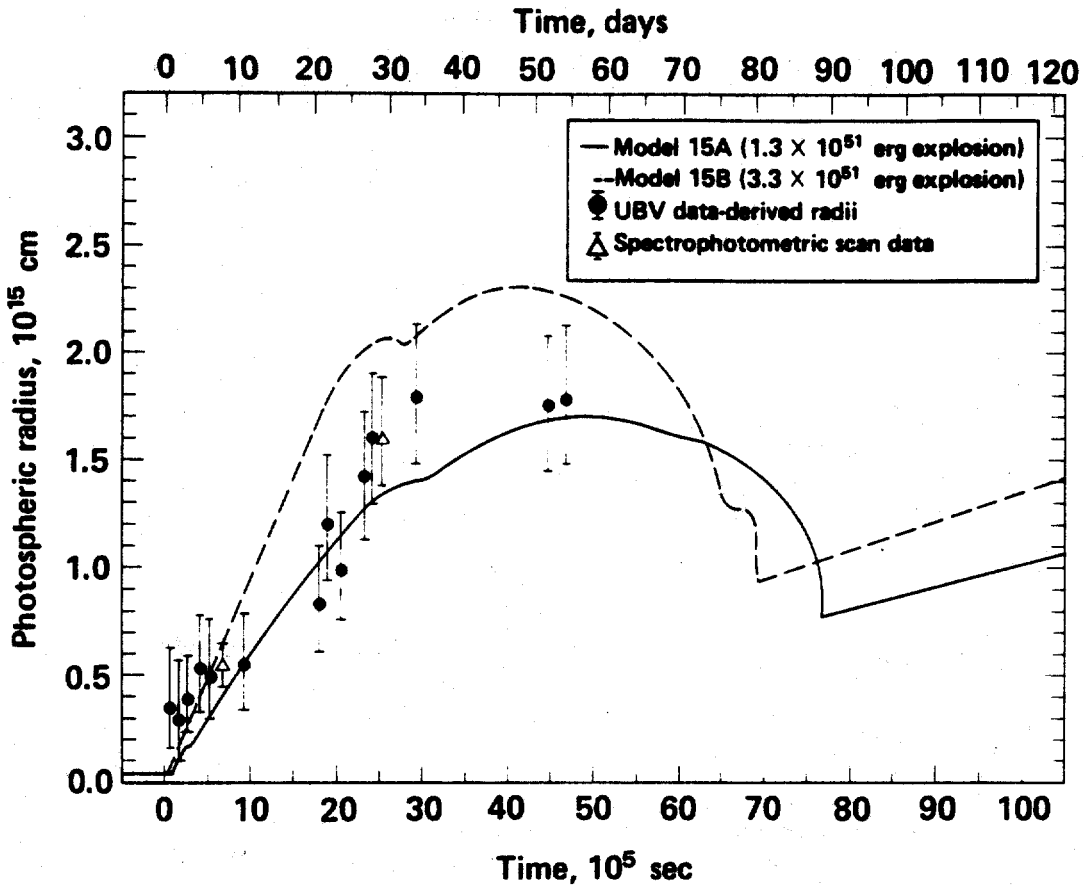

Fig. 7 Photospheric radius of Type II supernova 1969ℓ compared to 15 $M_\odot$ theoretical models.[6] Solid and dotted lines give the results for the 15 $M_\odot$ models, while the 1969ℓ data points are either derived from UBV data[18] or multifrequency scans.[2]

The star remains sufficiently optically thick during its acceleration that 99% of the total supernova energy is converted to kinetic energy of the expanding debris. Only about 1% thus remains to be radiated when the star finally starts to become optically thin after expanding to about 10^{15} cm, or about 10 to 30 times its initial radius. As Figure 5 illustrates, this division of energy is just sufficient to explain supernova observations of the SN 1969ℓ variety. Presupernova stars with radii much larger or much smaller than 3 to 7×10^{13} cm (corresponding to our 15 and 25 $M_\odot$ models) would respectively radiate too great or too small a fraction of the total supernova energy to agree with the observations.

The photosphere initially lies close to the outer surface of the star, and thus expands rapidly in physical size as the star explodes. Figure 9 shows the evolution of the density profile near the surface of the star during the first 20 days of the explosion, and the position of the photosphere is noted. It is apparent that after the first few days the density at a given mass coordinate scales as t^{-3} corresponding to an homologous expansion (velocity $\propto$ radius) with a frozen-out velocity distribution. The photosphere first moves outward

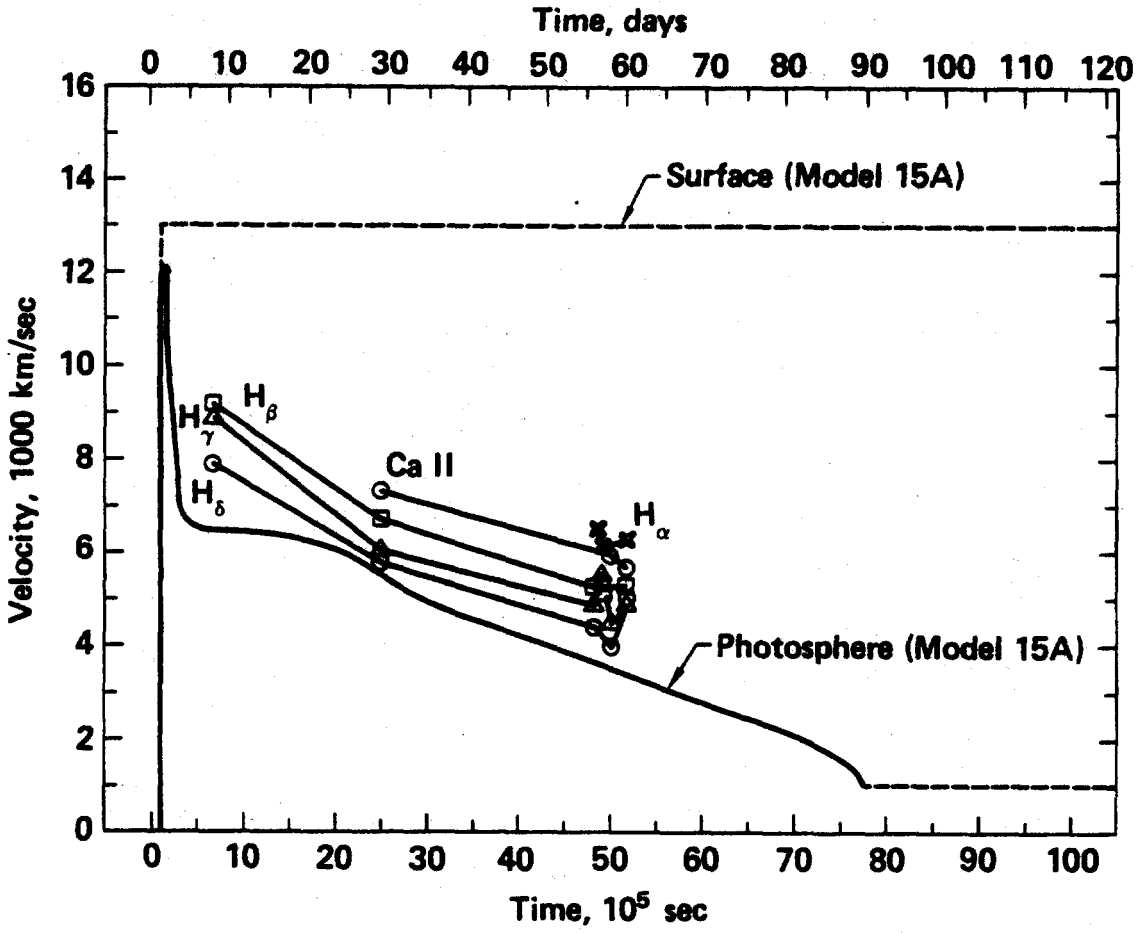

Fig. 8 Time evolution of the surface and photospheric velocities of the 1.3 x 10^{51} erg, 15 $M_\odot$ supernova model (15A) compared with absorption lines velocities observed[2] for supernova 1969ℓ.[6]

in mass coordinate from its presupernova position due to shock-induced reionization of the overlying material, and then moves inward with respect to the expanding envelope material maintaining an almost constant density of 10^{-13} g/cc.

After about 20 days, the photosphere has cooled to roughly 6000 K, the temperature at which hydrogen plasma recombines to form a nearly transparent atomic gas at the extremely low densities prevalent in the envelope. This recombination-induced transparency allows the rapid radiative cooling of the immediately underlying layers, causing them in turn to recombine and become transparent. A cooling wave thus develops that sweeps inward through the exploding envelope over a period of about two months. The photosphere follows the recombination front associated with this cooling wave, and thus its temperature remains close to the 6000 K recombination temperature (see Fig. 6). In addition, the radius of the photosphere remains nearly constant ($\approx$1.5-2.0 x 10^{15} cm) during this period because the inward motion of the photosphere relative to the envelope material is approximately canceled out by the overall expansion of the

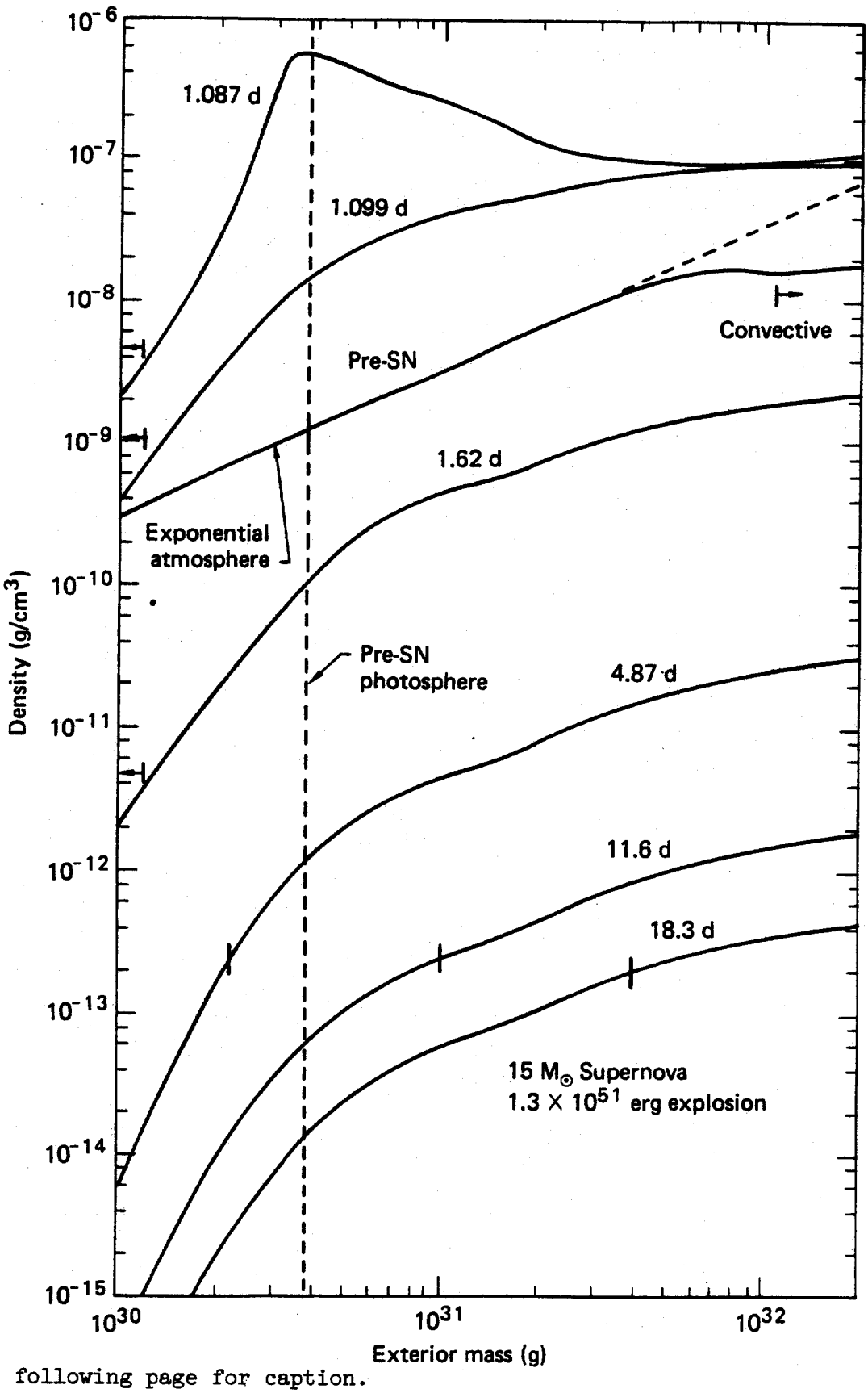

See following page for caption.

Fig. 9 (previous page) Density profiles as a function of exterior mass coordinate of the 1.3 x 10^{51} erg, 15 $M_\odot$ supernova model (15A) during the first 20 days of the explosion. The curves are labeled with the time since core collapse, and the position of the photosphere is indicated by a bar. The curve labeled "Pre-SN" is the presupernova density profile, which over most of the mass range shown has the form of an exponential atmosphere (dotted line). As indicated, the presupernova envelope is convective for exterior masses greater than 1.1 x 10^{32} g.

envelope. It is this combination of nearly constant photospheric radius and temperature that causes the supernova's luminosity to remain roughly constant during the plateau phase of the light curve (see Fig. 5).

Figures 10 and 11 illustrate the evolution of the temperature and density profiles during this epoch. Note that slight (possibly numerical) irregularities in the nearly homologous hypersonic flow have induced the growth of density spikes in the mantle.

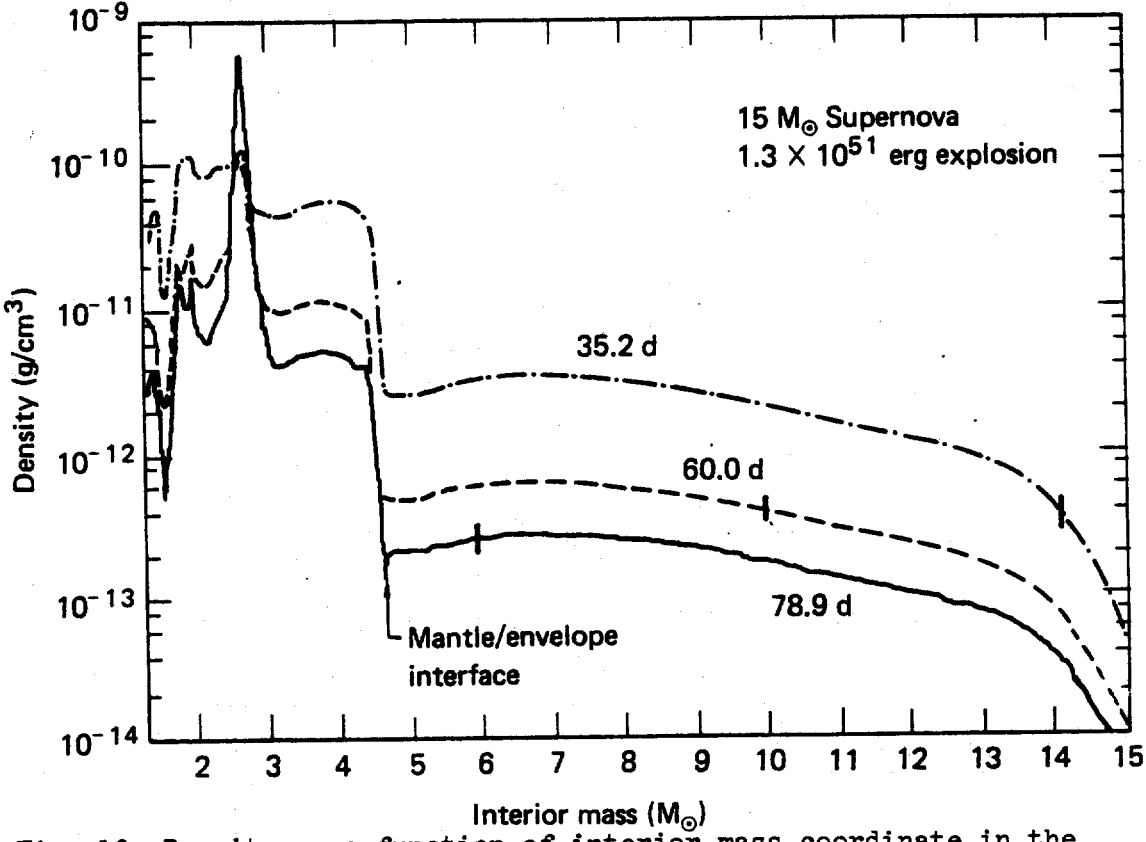

Fig. 10 Density as a function of interior mass coordinate in the 1.3 x 10^{51} erg, 15 $M_\odot$ supernova model during the transparency-wave-induced "plateau" epoch of its light curve. Each curve is labeled with the time since core collapse. The position of the photosphere is shown by the bar across each curve.

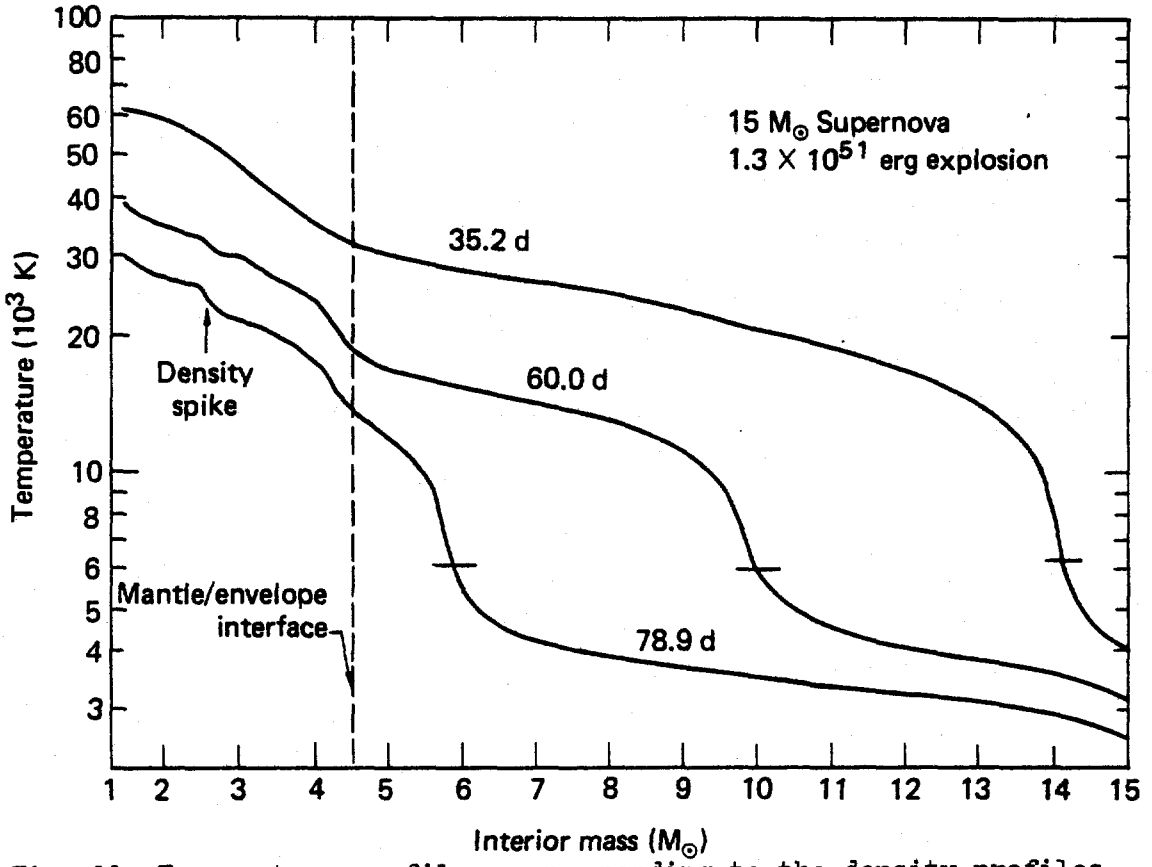

Fig. 11 Temperature profiles corresponding to the density profiles presented in Fig. 10. Again, the position of the photosphere is indicated by a bar.

Eventually, as the cooling wave encounters more slowly moving material deep within the envelope, the speed of the wave exceeds the matter velocity, and the photosphere physically shrinks until it encounters the slowly moving (<1000 km/s), relatively dense, and very optically thick mantle (see Fig. 7). At this point, a transient increase in the photospheric temperature occurs and persists for approximately two to three days as a result of the uncovering and rapid cooling of the hot surface of the mantle. This phenomenon is potentially observable, although the presence of strong emission lines in the overlying envelope may tend to mask it. The sharpness of this final recession and the resulting decrease in luminosity probably are artificially abrupt because of our relatively simplified treatment of recombination and emission-line effects.[5]

At late times, the luminosity results from the diffusion out of the mantle of thermalized radiation from the decay of the explosively generated ^{56}Ni and its daughter ^{56}Co. As Figure 5 shows, models in which ^{56}Ni decay is turned off display a much more sharply falling luminosity tail as the residual thermal energy in the mantle diffuses out over a characteristic time of only one to two months. In models containing energy output from radioactivity, temporary trapping of the thermalized decay energy in the optically thick mantle produces a luminosity decline slower than the 78-day ^{56}Co half-life, particularly in the 25 $M_\odot$ case.

The deposition of the positrons and γ-rays from these decays takes place almost entirely in the mantle due to the large column density of overlying material that is present even at very late times, as shown in Figure 12. As expected, the column density at a given mass coordinate scales as t^{-2} due to the nearly homologous expansion of the star.

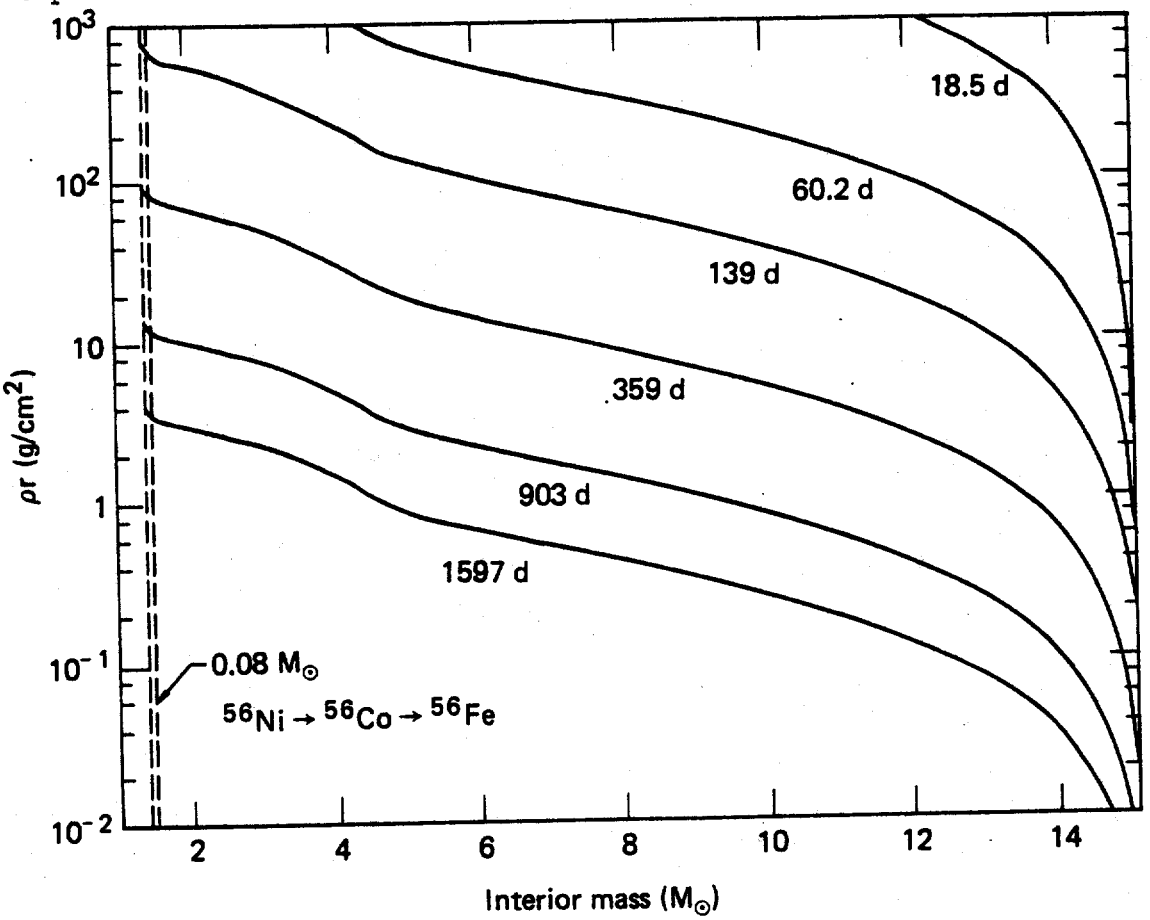

Fig. 12 Column density, ρr, of overlying material as a function of interior mass coordinate in the 1.3 x 10^{51} erg, 15 $M_\odot$ supernova model. Each curve is labeled with the time since core collapse, and the position of the 0.08 $M_\odot$ of ^{56}Ni formed in the explosion is indicated.

The peak emission of unscattered γ-rays takes place at about 400 days and yields a peak flux in the 3.2 MeV line of about 5 x 10^{-5} photons $cm^{-2}sec^{-1}MeV^{-1}$ (see Ref. 26) for the 1.3 x 10^{51} erg, 15 $M_\odot$ supernova model, assuming a distance of 1 Megaparsec.

The ripples in the theoretical curves at late times result from the formation of density clumps in the mantle noted earlier, which if real appear to offer excellent sites for grain formation. It is likely that two-dimensional instabilities will also occur[14] (as is suggested by the clumpy appearance of supernova remnants) which should have the effect of increasing the noise, but damping the size of the transient excursions in the luminosity.

In principal, a great deal of information about supernova can be deduced from their light curves. At times earlier than 3 months, the light curve principally conveys information about the structure of the envelope of the presupernova star. More massive, extended envelopes produce prolonged luminosity plateaus and slower photospheric velocities for fixed shock energies. The behavior of the tail of the light curve, on the other hand, yields information about the size and density of the mantle, and ultimately, its composition.

In order to realize the full potential of these sources of information for understanding supernovae and the elements they produce, it will be necessary to perform detailed calculations of non-LTE supernova atmospheres so that spectral information about composition and plasma conditions can be unfolded. It is hoped that the Type II supernova models presented here will provide a starting point for, and help to motivate such work, as well as extensive new observations of supernovae. Taken together, such advances should allow the confident use of supernovae as both standard[27-28] and "non-standard candles"[18,21,29] for determining distances to distant galaxies.

EDGE-LIT CARBON DETONATIONS OF ACCRETING WHITE DWARFS AS TYPE I SUPERNOVAE

Since this workshop is primarily concerned with Type I supernovae, it seems irresistable to broaden the topic of this talk to very briefly describe some of our recent calculations of the fate of white dwarfs undergoing slow mass accretion. A more detailed description will be published elsewhere.[30]

Our calculations were started from an initial model supplied by Taam[31] in which a 0.5 $M_\odot$ white dwarf composed of equal concentrations of carbon and oxygen accretes hydrogen (assumed burned quickly to helium) at a rate of 10^{-8} $M_\odot$ yr^{-1} until 0.62 $M_\odot$ of helium has accumulated. The star's density and temperature profiles at this stage are shown in Figure 13. At this point, electron conduction cooling, which has allowed the helium to form a highly degenerate layer on the surface of the star ($\rho \sim 10^7$ g/cc, T~5 x 10^7 K) is no longer sufficient to counteract the compressional heating of the star due to the increasing overlying mass of helium, and a thermonuclear runaway results at the carbon/helium interface.

Using the stellar evolution/explosion code described above to follow this star's subsequent evolution, we found that, after a brief phase of convective helium burning, the overpressure from the nuclear runaway induces shock waves propagating both outward through the helium layer and inward through the carbon-oxygen core. These shocks ignite further nuclear burning and are rapidly transformed into self-sustaining Chapman-Jouguet detonation waves. The burning fuel is sufficiently inertially confined so that the final product is predominantly ^{56}Ni. The ease with which carbon is ignited in this manner, in contrast to the still unresolved difficulties[32,33] associated with the central ignition of carbon in white dwarfs near the Chandrasekhar mass, is a direct consequence of the 2-3 order-of-magnitude reduction in ignition density in the present case which makes possible nuclear-burning-induced overpressures of ~400%, instead of ~20-50%.

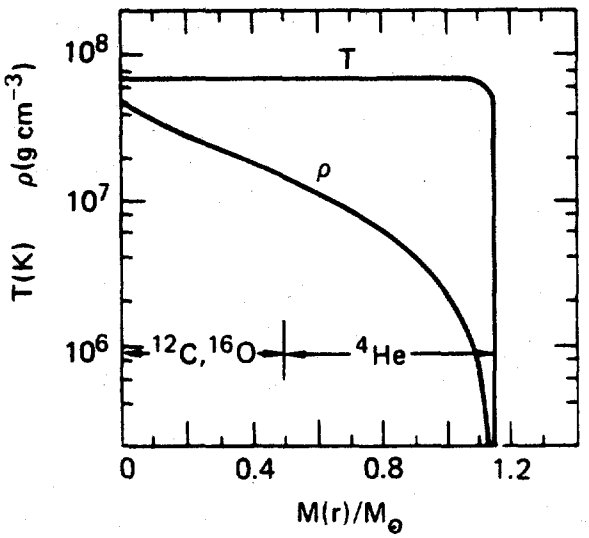

Fig. 13 Density (ρ) and temperature (T) as a function of interior mass coordinate (M(r)/M$_\odot$) in the initial white dwarf model of Taam[31] just prior to He ignition.

The present status of this calculation is illustrated in Figure 14 which shows the diverging He and C/O nuclear detonation waves just before they reach the surface and center of the star, respectively. Preliminary extensions of this calculation suggest that the light curve and velocities characteristic of Type I supernovae may result as the ≈1 M$_\odot$ of ^{56}Ni synthesized by the detonation, and expands and decays.

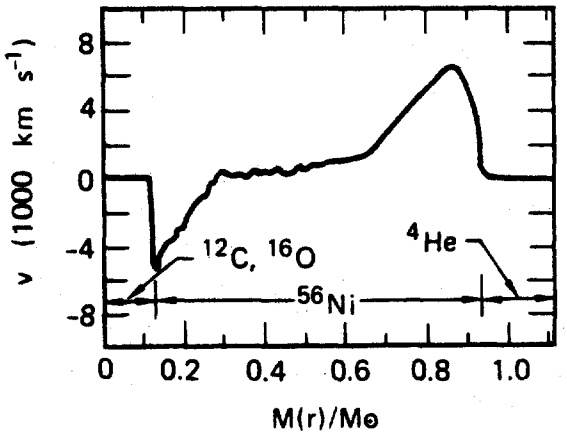

Fig. 14 Velocity and composition profiles of the detonating white dwarf model.

A possible complication is that the He will most likely runaway at a point instead of along an entire spherically symmetric mass shell (as we are forced to assume), resulting in a detonation wave propagating spherically outward from a point offset with respect to the center of the star. Generic two-dimensional investigations of off-center detonations by Fryxell[34] suggest, however, that provided the detonation can still progagate against the initially higher rate of geometric divergence, the final state of the detonated star should be nearly the same.

Ron Taam is gratefully acknowledged for supplying details of his accreting white dwarf models prior to publication and for useful discussions.

REFERENCES

1. R. Minkowski, Annual Reviews, 2, 247 (1964).
2. R. P. Kirshner, J. B. Oke, M. V. Penston, and L. Searle, Ap. J. 185, 303 (1973) and references cited therein; R. P. Kirshner, and J. B. Oke, Ap. J. 200, 574 (1975).
3. I. S. Shklovsky, Supernovae (Wiley, New York, 1968), p. 20.
4. J. Maza and S. van den Bergh 204, 519 (1976).
5. T. A. Weaver, G. B. Zimmerman, and S. E. Woosley, Ap. J. 225, 1021 (1978). Also see references therein.
6. T. A. Weaver and S. E. Woosley, Proc. 9th Texas Symposium on Relativistic Astrophysics, Munich, 1978, Ann. N.Y. Acad. Sci. 336, 335 (1980).
7. T. A. Weaver and S. E. Woosley (1980), in preparation.
8. S. E. Woosley and T. A. Weaver (1980), in preparation.
9. E. M. Burbidge, G. R. Burbidge, W. A. Fowler, and F. Hoyle, Rev. Mod. Phys. 29, 547 (1957).
10. J. R. Wilson and R. L. Bowers (1978), private communication; J. R. Wilson, Proc. 9th Texas Symposium on Relativistic Astrophysics, Munich, 1978, Ann. N.Y. Acad. Sci. 336, 358, (1980).
11. Ya. B. Zel'dovich and Yu. P. Raizer, Physics of Shock Waves and High-Temperature Hydrodynamic Phenomena (Academic, New York, 1966), p. 93.
12. G. E. Miller and J. M. Scalo, Ap. J. Suppl. 41, 513 (1979).
13. R. A. Chevalier, Ap. J. 207, 872 (1976).
14. R. A. Chevalier and R. I. Klein, Ap. J. 219, 931 (1978).
15. G. J. Lasher, Ap. J. 201, 194 (1975), and this conference.
16. F. L. Ciatti, L. Rosino, and F. Bertola, Mem. Soc. Astron. Ital. 42, 163 (1971).
17. R. Barbon, F. Ciatti, and L. Rosino, Astron. & Astrophys. 29, 57 (1973).
18. R. P. Kirshner and J. Kwan, Ap. J. 193, 27 (1974).
19. S. W. Falk and W. D. Arnett, Ap. J. Lett. 180, L65 (1973); S. W. Falk and W. D. Arnett, Ap. J. Suppl. 33, 515 (1976).
20. W. D. Arnett and S. W. Falk, Ap. J. 210, 733 (1976).
21. S. R. Schurmann, W. D. Arnett, and S. W. Falk, Ap. J. 230, 11 (1979).
22. E. K. Grassberg, V. S. Imshennick, and D. K. Nadyozhin, Astrophys. Space Sci. 10, 28 (1971).
23. G. J. Lasher and K. L. Chan, Ap. J. 230, 742 (1979).
24. R. I. Klein and R. A. Chevalier, Ap. J. Lett. 223, L109 (1978).
25. R. A. Chevalier and R. I. Klein, Ap. J. 234, 597 (1979).
26. T. S. Axelrod, private communication (1980).
27. L. Rosino, in Supernovae, ed. D. N. Schramm (Reidel, Dordrecht-Holland, 1977), p. 1.
28. L. Rosino and G. Di Tullio, in Supernovae and Supernova Remnants, ed. C. B. Cosmovici (Reidel, Dordrecht-Holland, 1974), p. 19.

29. D. Branch, in Supernovae, ed. D. N. Schramm (Reidel, Dordrecht-Holland, 1977), p. 21; R. V. Wagoner, Ap. J. Lett. 214, L5 (1977).
30. S. E. Woosley, T. A. Weaver, and R. E. Taam (1980), in preparation.
31. R. E. Taam, Ap. J. 237, 142 (1980) and references therein; and private communication (1979).
32. R. G. Couch and W. D. Arnett, Ap. J. 196, 791 (1975); S. W. Bruenn and A. Marroquin 195, 567 (1975) and references therein.
33. J. C. Wheeler, J-R. Buchler, and Z. K. Barkat, 184, 897 (1973); D. Sugimoto and K. Nomoto, preprint (1979), and references cited therein.
34. B. A. Fryxell, Ap. J. 234, 641 (1979).

NOTICE